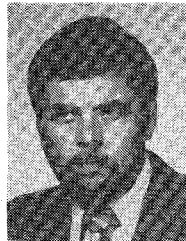


wards the Ph.D. degree in electronics at the Research Institute of Electronics, Shizuoka University, Hamamatsu, Japan, where he is primarily involved in microwave solid-state oscillators design and power-combining schemes.

Mr. Madhian is a member of the Institute of Electronics and Communication Engineers of Japan.



Andrzej Materka was born in Leczyca, Poland, on November 18, 1949. He received the M.Sc. degree in radio engineering from Warsaw Technical University and the Ph.D. degree in technical sciences from Lodz Technical University in 1972 and 1979, respectively.

From 1972 to 1974 he worked for the Radio and Television Broadcasting Stations, Lodz, Poland, on transmitters and circuits for space division of video signals. Later, he joined the Institute of Electronics, Lodz Technical University, to serve as a Research and Teaching Assistant on testability of analog circuits, CAD design, and semiconductor devices modeling. Since 1979 he has been a Lecturer at the same university.

In 1980 he was granted a Japanese Government scholarship and joined the Research Institute of Electronics, Shizuoka University, Hamamatsu,

Japan. His current research interests include power combining techniques and FET oscillators.



Shizuo Mizushima (S'60-M'66) was born in Hamamatsu, Japan, on August 10, 1933. He received the B.Eng. degree from Shizuoka University, Hamamatsu, in 1957, and the M.Sc. and Ph.D. degrees from Ohio State University, Columbus, in 1962 and 1964, respectively.

From 1957 to 1960 he was a Research Assistant and Lecturer at Shizuoka University. From 1964 to 1965 he was a Member of the Technical Staff at the Bell Telephone Laboratories, Murray Hill, NJ. In 1965 he returned to Shizuoka University where he is now a Professor at the Research Institute of Electronics. He has worked on millimeter-wave magnetrons, gigabit-pulse regenerators, solid-state oscillators, and device-circuit interaction problems. His current research interests are concerned with microwave power-combining techniques, microwave thermography, and medical electronics.

Dr. Mizushima is a member of the Institute of Electronics and Communication Engineers of Japan, the Japan Society of Medical Electronics and Biological Engineering, and Sigma Xi.

Thermally Induced Switching and Failure in p-i-n RF Control Diodes

ROGER J. CHAFFIN, SENIOR MEMBER, IEEE

Abstract—This paper measures and analyzes a thermally induced, breakdown-like effect in p-i-n RF switching diodes. The effect is found to be due to thermally generated carriers increasing the *I*-region conductivity and loss. This is a positive feedback situation which, with increasing power levels, eventually causes the diode to switch to a low-impedance state. In the low-impedance state, further increases in temperature have a negative feedback effect on the absorbed power and hence this mode is stable with a very large hysteresis effect. Unfortunately, the high temperatures encountered in the low-impedance mode ($\sim 400^\circ\text{C}$) have a detrimental effect on diode reliability. The threshold power at which switching to this mode occurs can be increased somewhat by reverse biasing the diode or improving its heat sink.

I. INTRODUCTION

RECENT, APPARENTLY unexplained, failures in a 500-MHz p-i-n switching diode (HP 5082-3081) in a receiver front-end caused us to investigate this problem. It

Manuscript received February 22, 1982; revised June 30, 1982. This work was supported in part by the U.S. Department of Energy under Contract DE-AC04-76DP00789.

The author is with Sandia National Laboratories, Albuquerque, NM 87185.

was found that even when the diode was reverse biased, coupling of a few watts of power from a nearby CW transmitter would cause the diode to switch to a stable, high temperature, low-impedance state. The temperatures in this state ($\sim 400^\circ\text{C}$) caused diode failure due to melting of the chip bond solder joint. Experimental and theoretical investigations of this effect are described in this paper.

II. EXPERIMENT

The diode, an axial lead, glass packaged device, has an *I*-region width of $\sim 175 \mu$ and a cross-sectional area of $\sim 4.9 \times 10^{-4} \mu^2$. The breakdown voltage is > 100 V with an allowable dissipation of 250 mW at 25°C . The diode was placed at the end of a 50Ω transmission line and connected through a network analyzer to a variable power 50Ω generator at 500 MHz. In the first test the diode was held at zero bias by a dc-return choke. Fig. 1 shows the measured results versus applied RF power. Fig. 1(a) and (b) show that as the power is initially increased from zero, the diode impedance is $\gg 50 \Omega$ ($|S_{11}| \sim 0 \text{ dB}$, $< S_{11} \sim 0^\circ$).

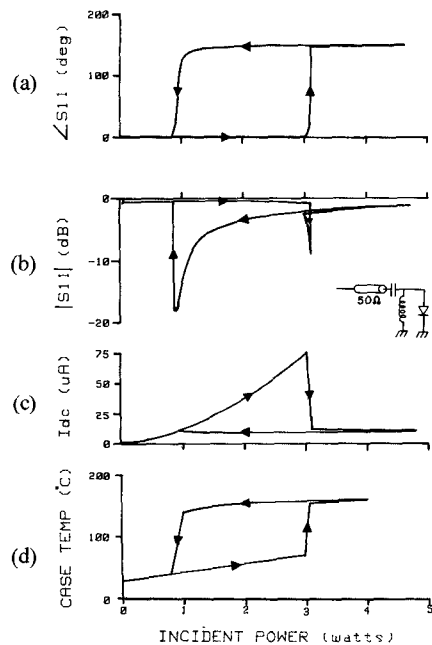


Fig. 1. Thermal breakdown in dc-shorted p-i-n diode. (a) Angle of reflection coefficient. (b) Magnitude of reflection coefficient. (c) Self rectified current. (d) Diode case temperature. Horizontal scale is incident RF power at 500 MHz.

At about 3 W of applied power, a sharp "dip" is seen in the $|S_{11}|$ and the angle changes to $\sim 150^\circ$, for further increases in power the $|S_{11}|$ stays near 0 dB with an angle of $\sim 150^\circ$. This is a low impedance ($\ll 50 \Omega$) state. As the power is reduced, an appreciable hysteresis can be seen and finally at ~ 0.9 W a sudden transition back to the high-impedance state is seen. The "dips" in $|S_{11}|$ occur at two power levels, near 3 W as the power is being increased, and near 1 W as the power is reduced. The "dip" at 3 W is not stable and cannot be held, but the "dip" at 1 W is stable. Fig. 1(c) and (d) help to explain the effect. Fig. 1(c) shows that the self rectified current initially increases with applied power and this of course decreases the diode impedance towards 50Ω . Fig. 1(d) shows the glass case temperature of the diode (lower than the actual chip temperature). At the switching point near 3 W, a dramatic jump in chip temperature is seen and this new value remains until the power is reduced below ~ 0.9 W. It was also found that the breakdown power threshold could be increased by blowing a jet of compressed air on the diode package.

In the second experiment, the applied bias conditions were changed and $|S_{11}|$ measured versus applied power. Note—this test was for a different diode of the same type (HP 5082-3081). (The first device failed after a few cycles of the test shown in Fig. 1.) In this test, the switching to the low-impedance mode occurs at 2.9 W (open circuit), 2.1 W (dc shorted), and 3.6 W (-5 V bias) and the same hysteresis effect occurs in all cases. The most striking observation from Fig. 2 is that the diode thermal breakdown occurs even at open circuit when no self rectified current can flow! This result was repeated with all other diodes tested, i.e., all diodes showed thermal breakdown in the 2–4-W applied power range, even when open circuited.

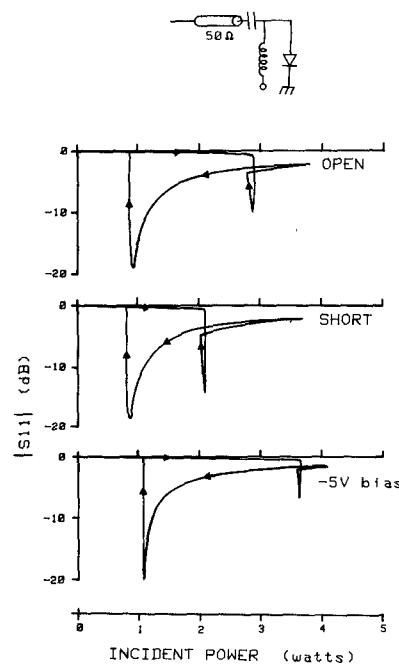


Fig. 2. Magnitude of reflection coefficient versus incident 500-MHz power for different diode bias conditions.

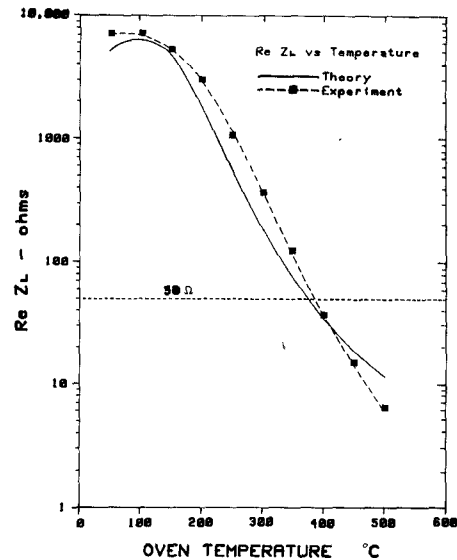


Fig. 3. Real part of diode impedance for open-circuit biased p-i-n diode versus temperature. Theory is solid line, measured value is dashed line (small signal measurement).

This finding prompted a further experiment. In this experiment, the diode was placed in a variable temperature oven and its dc open-circuit impedance was measured with a small < 10 -mW RF signal at 500 MHz. Under these conditions the entire diode is expected to be at a uniform temperature equal to the oven temperature. Fig. 3 shows the real part of the unbiased diode impedance versus oven temperature. The figure shows a steady decline in diode impedance with increasing temperatures, passing through 50Ω at 385°C . Therefore, it is concluded that with large applied powers, a small dissipation occurs even in the unbiased diode I region, probably due to resistance experienced by the injected (and recovered) carriers that flow

during each RF cycle, even though no net current can flow. This dissipation causes diode heating and subsequent thermal breakdown as seen earlier.

III. THEORY

A simplified p-i-n diode structure is shown in Fig. 4(a). The basic principle of operation used is to place the diode in shunt or in series with a transmission line. When the diode is zero or reverse biased, it is a very high impedance, and when it is forward biased, it is a very low impedance due to conductivity modulation of the *I* region. The equivalent circuit, at zero bias, is shown in Fig. 4(b). The resistance of the *I* region dominates the characteristics of the diode for the effects discussed in this paper, hence Fig. 4(c) is the simplified equivalent circuit of interest. The conductivity of the *I* region can be calculated from

$$\sigma_i = ne\mu_e + pe\mu_h$$

where

$$e = 1.6 \times 10^{-19} \text{ Coulomb}$$

$$p = n = n_i + n_0$$

μ_e, μ_h = electron, hole mobility

$$n_0 = \text{fixed background doping} \sim 3 \times 10^{13} \text{ cm}^{-3}.$$

The intrinsic carrier density n_i will vary as $\sim 10^{16} T^{3/2} \exp(-E_g/2kT)$, where E_g = bandgap and k = Boltzmann's constant. The effects of bandgap narrowing must be included in E_g [1]. The mobility can be approximated [2] as

$$\mu_e = 2.1 \times 10^9 T^{-2.5}$$

$$\mu_h = 2.3 \times 10^9 T^{-2.7}$$

T = temperature K.

Using the carrier density and the mobility equations above, the conductivity of the *I* region σ_i can be calculated. If we assume the *I* region has the form of a slab 175μ thick with an area of $4.9 \times 10^4 \mu^2$, the resistance of the *I* region will be given by

$$R_i \cong \frac{36}{\sigma_i}, \quad \text{where } \sigma_i \text{ is in } (\Omega \cdot \text{cm})^{-1}.$$

This theoretical value has been plotted in Fig. 3 and can be seen to be in good agreement with the measured value of R_i versus temperature. The important thing to note is that Fig. 3 will represent the diode impedance with no applied or self rectified bias current. Hence, the explanation of the effect seen in Figs. 1 and 2 is that as the diode absorbs power and heats up, its *I*-region resistance drops until it absorbs all of the incident power at $R_i \cong 50 \Omega$. Its resistance will continue to drop due to heating, reducing the absorbed power until a steady state is reached where a further decrease in the impedance reduces the absorbed power. The absorbed power is given by

$$\frac{P_{\text{abs}}}{P_{\text{inc}}} = 1 - |S_{11}|^2 \cong 1 - \left(\frac{R_i - 50}{R_i + 50} \right)^2. \quad (1)$$

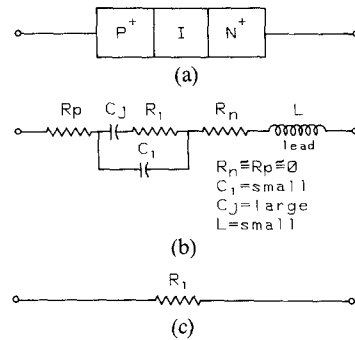


Fig. 4. Equivalent circuit of p-i-n diode. (a) Diode cross section. (b) Detailed equivalent circuit. (c) Simplified equivalent circuit at 500 MHz.

The *I* region temperature rise will be given by

$$\Delta T = \Theta \cdot P_{\text{abs}} \quad (\Theta = \text{thermal impedance}). \quad (2)$$

Figs. 1 and 2 show that after thermal switching, the diode impedance stays below 50Ω down to about 1 W of incident power. At that point the sharp dip in S_{11} indicates it is passing through the 50Ω point and $P_{\text{inc}} = P_{\text{abs}}$ (see (1)). From Fig. 3 we can estimate the *I*-region temperature for $R_i = 50 \Omega$ in an unbiased diode as 390°C . Therefore, at $P_{\text{abs}} = 1 \text{ W}$, $\Delta T = 390 - 25$ (ambient) = 365°C , and from (2) we find $\Theta = 365^\circ\text{C}/\text{W}$. Equations 1 and 2 may now be combined to yield

$$\Delta T \cong 365 \cdot \left[1 - \left(\frac{R_i - 50}{R_i + 50} \right)^2 \right] \cdot P_{\text{inc}}. \quad (3)$$

This equation gives the relation between the *I*-region temperature and the incident power. For example, at $T = 500^\circ\text{C}$ ($\Delta T = 475^\circ\text{C}$), $R_i \cong 6 \Omega$ (from Fig. 3) and hence $P_{\text{inc}} = 3.4 \text{ W}$. Thus, for 3.4 W of incident power we expect an *I*-region temperature of 500°C for an unbiased diode.

The preceding calculations support the earlier comments about the negative feedback effect of this breakdown mode, i.e., for changes of P_{inc} by a factor of 3.4 (from 1 W to 3.4 W) the temperature rise ΔT only changes by a factor of 1.3 (365°C to 475°C).

These high temperatures are certainly the cause of the premature failures in these devices discussed in the introduction of this paper.

A. Cure

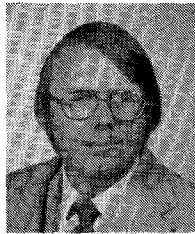
There is no simple cure for this problem without changing diode type. The most obvious solution to prevent damage to devices exposed to occasional high powers is to use a better heatsink for the diode, i.e., a stud mount instead of the axial lead package. An order of magnitude decrease in thermal impedance Θ would allow the device to handle an order of magnitude more power before breaking down. Increasing the reverse bias to fully deplete the *I* region is impractical for these wide-based p-i-n diodes, edge breakdown will occur long before the *I* region is depleted. However, a narrow-base p-i-n diode (such as a step recovery diode) could be fully depleted before breakdown and may be preferable for these applications.

ACKNOWLEDGMENT

The author would like to thank R. A. Hibray of Sandia National Laboratories for his assistance in this study.

REFERENCES

- [1] S. M. Sze, *Physics of Semiconductors*. New York: Wiley Interscience, 1969, p. 24.
- [2] J. L. Moll, *Physics of Semiconductors*. New York: McGraw-Hill, 1964, p. 197.



Roger J. Chaffin (M'67-SM'78) received the B.S., M.S., and Ph.D. degrees in electrical engineering from the University of Wisconsin, Madison.

He joined Sandia National Laboratories, Albuquerque, NM, in 1967 and is currently the Supervisor of the Solid-State Device Physics Division (Division 5133), where his work involves research on optoelectronic and microwave devices. He is the author of numerous publications on microwave devices, including *Microwave Semiconductor Devices*, published by Wiley Interscience.

Wave Propagation in Inhomogenous Slab Waveguides Embedded in Homogenous Media

AKIRA YATA AND HIROYOSHI IKUNO

Abstract—Wave propagation in inhomogeneous slab waveguides embedded in homogeneous media is analyzed by using the uniform asymptotic technique. This technique accurately evaluates the effect of the refractive-index profiles with various core and cladding structures on the guided modes. We calculate the guided modes of waveguides with asymmetric claddings in the cases of a near-parabolic profile core and a quasi-Gaussian profile core. The results show that the third-order asymptotic solution is accurate for all the guided modes in the case of the near-parabolic profile core and for modes far from cutoff in the quasi-Gaussian core case. The dispersion relation indicates that modes guided in strongly asymmetric profiles have almost the same propagation constants as odd-order modes of propagation in the symmetric structure.

I. INTRODUCTION

ADVANCES OF integrated optics produce optical channel waveguides and directional couplers with a great variety of refractive-index distributions. In such waveguides, propagation characteristics of the guided modes are strongly influenced by the inhomogeneous core and the uniform cladding. A number of numerical methods are used for evaluating the effect of the structure on guided modes [1]–[4]. A more efficient analytic method is desired for studying the wave propagation in a typical Gaussian slab waveguide structure.

The uniform asymptotic method developed in a companion paper [5] is a useful approximate technique for analyzing the guided modes of a considerably general class of refractive-index profiles. We derive an expression for calculating the third-order correction to the WKB solution of the guided modes of the uncladded waveguide in which the core variety is described by an even polynomial refractive-index profile. When considering the cladded waveguides, we need to replace the *integer mode index* of the ideal waveguide eigenvalues and modal fields with the *non-integer mode index*. The unknown non-integer mode index is determined by solving the characteristic equation which is derived from the boundary conditions at the core-cladding interfaces. In this formulation, the cladding effect is automatically included in the non-integer mode index [6], [7]. The method presented here is a uniform asymptotic approach in the sense that the modal field distributions of the waveguide with various refractive-index profiles are obtained in all orders for all points across the cross section.

As an actual example, we calculate the third-order approximate solution of the non-integer mode index in the case of the asymmetric refractive-index distribution. The convergence and the accuracy of the solutions are checked numerically in two cases; the near-parabolic profile core and the quasi-Gaussian profile core. Lastly, we examine

Manuscript received March 4, 1982; revised April 28, 1982.

The authors are with the Department of Information Engineering, Kumamoto University, Kumamoto 860, Japan.